

# Jamming Mechanisms and Density Dependence in a Kinetically-Constrained Model

Yair Shokef<sup>1</sup> and Andrea J. Liu<sup>2</sup>

<sup>1</sup>Department of Physics of Complex Systems, Weizmann Institute of Science, Rehovot 76100, Israel

<sup>2</sup>Department of Physics and Astronomy, University of Pennsylvania, Philadelphia, PA 19104, USA

(Dated: October 19, 2019)

We generalize a kinetically-constrained lattice-gas model to explore the jamming phase-diagram of the system as a function of density, temperature and non-equilibrium driving. We add temperature and driving to the recently-proposed spiral model which jams at a critical density smaller than 1. In this way we can access unjamming by temperature or driving at densities above the critical density. We numerically calculate the relaxation time of the persistence function and its spatial heterogeneity. We manage to disentangle the relaxation mechanisms responsible for unjamming along different paths in the phase diagram and show that the spatial scale of dynamic heterogeneities is much more strongly dependent on density than on temperature and driving.

PACS numbers: 64.70.Q-, 05.70.Ln, 45.70.-n, 47.57.-s

Glass-forming-liquids, colloids, emulsions, foams, and granular materials all develop sluggish and heterogeneous dynamics as they approach the onset of jamming. The slowing down of the dynamics in these systems with increasing density of the constituent particles, decreasing temperature, or decreasing external mechanical driving is often summarized in the form of a jamming phase-diagram [1]. To date, most numerical studies of the jamming phase-diagram have focused on particulate models such as sphere packings. From a theoretical point of view, however, simpler models can be easier to understand. In this Letter, we introduce a lattice model with a phase-diagram (Fig. 1A) that is similar to that of sphere packings. We show that the interplay of density, temperature, and driving in this model can be sorted out and understood, and suggest that the resulting insights may be applicable to more realistic systems.

In the limit of zero temperature and driving, ideal sphere packings undergo a jamming transition at random-close-packing [2]. The transition at this so-called Point J has a mixed nature in that the number of interacting neighbors per sphere *jumps discontinuously* from zero below Point J to the minimum number needed for mechanical stability above the transition, but there is a *diverging time-scale* [3, 4]. Above the critical density, the spheres may be unjammed either by raising temperature above a glass transition into an equilibrium state or by applying a shear stress above a yield stress to drive the system into a homogeneous non-equilibrium steady-state.

To construct a lattice model with a phase diagram similar to that of sphere packings, we start with a kinetically-constrained lattice-gas as a zero-temperature model. In such models, occupied sites do not interact but the dynamical rules governing changes in occupation of a site depend on the occupation of neighboring sites. This leads to dynamics that are increasingly slow and heterogeneous as the fraction  $\rho$  of occupied sites increases, since increasingly larger regions are required to rearrange collectively [5]. Here we focus on the spiral model [6], see Fig. 1B, which jams into a non-ergodic phase at a critical density  $\rho_c \approx 0.705$ . This allows us to study its behavior at  $\rho > \rho_c$  with nonzero temperature or driving. Such jamming-percolation models [7, 8] possess an additional im-

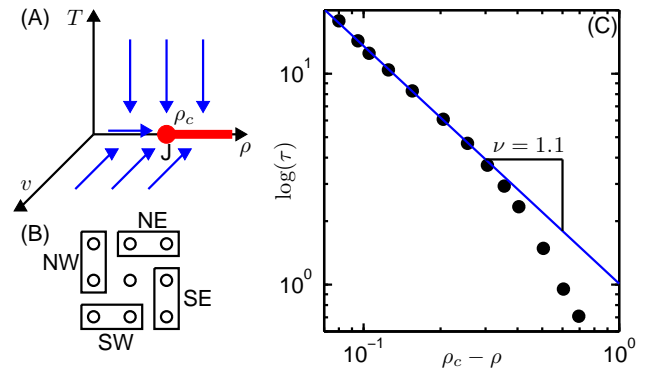


FIG. 1: (Color online) A) Jamming phase diagram of density  $\rho$ , temperature  $T$ , and driving  $v$ . Jammed phase is the thick red line along the  $\rho$ -axis which terminates at Point J. Blue arrows are the trajectories we investigate. B) The spiral model is defined such that the occupation of a site on the square lattice can change if its (NE or SW) and (NW or SE) neighboring pairs are completely empty. C) Divergence of relaxation time as  $\rho \rightarrow \rho_c$  for  $T = 0$  and  $v = 0$ .

portant property from our point of view: the jamming transition at  $\rho_c$  has a mixed nature reminiscent of that of Point J. The fraction of stuck particles that cannot participate in rearrangements jumps discontinuously as in a first-order transition, while time and length scales diverge as in a second-order transition.

Kinetically-constrained models typically have a single control variable which is usually associated with temperature. In this interpretation, each site may be in one of two Ising states, representing active and inactive regions, such that the tendency to be active increases with temperature. The kinetic constraint limits the ability of a site to change from active to inactive and vice versa depending on its local environment. Alternatively, each site may be viewed as occupied or unoccupied so that the number of occupied sites increases with density, rather than temperature. We adopt this lattice-gas point of view, so that the dynamical slowing down in our version occurs with increasing density rather than decreasing temperature. The spiral model is defined as an Ising model with spin-flip dynamics, so that the number of particles is not conserved.

We therefore first modify the zero-temperature dynamics so that instead of flipping spins (or switching sites between being occupied and vacant) we move a particle to a neighboring site if the target site is vacant and if the kinetic constraint described in Fig. 1B holds both before and after the move. Time is measured in units of attempted moves per particle.

We introduce temperature by softening the kinetic constraints. Instead of preventing blocked moves, we allow them with probability  $\exp(-1/T)$ . Thus, for  $T = 0$  we recover the original model with rigid constraints. Note that the system still has no interactions and that energy is not associated with its different states but only with the virtual barrier the system has to cross in a kinetically-constrained move. For  $\rho > \rho_c$ , the system is non-ergodic only at  $T = 0$ , since for arbitrarily low temperature, kinetically-constrained moves occur at a slow but nonzero rate. As a result, the system may reach any configuration after a sufficiently long time for any  $T > 0$ .

We drive the system into a non-equilibrium steady-state by inducing a current of particles in one direction (for example, from left to right), as follows. In addition to the aforementioned moves in which particles can move into neighboring vacant sites subject to the soft ( $T > 0$ ) or rigid ( $T = 0$ ) kinetic constraint, we introduce a second type of move, in which a particle can move into the neighboring site to its right if it is vacant, irrespective of the kinetic constraints [9]. Such moves are attempted at rate  $f$ , and we characterize the driving strength by the average flow velocity  $v = (1 - \rho)f$  induced by them. Note that even for arbitrarily slow driving, the environment of any blocked particle will eventually change such that the particle will no longer be blocked and can move even under the kinetically-constrained dynamics [12].

The system is truly jammed only along the red line in Fig. 1A. However, if one uses the experimental definition of a glass and considers the system as jammed once the relaxation time exceeds a certain threshold, then there would be a jammed region in this phase diagram that extends with increasing density in this phase diagram that extends with increasing density to higher temperatures and driving strengths.

We study the generalized model numerically using rejection-free Monte-Carlo simulations on two-dimensional  $80 \times 80$  square-lattice systems. Results were found to be numerically convergent with system size by comparing to  $400 \times 400$  and  $2000 \times 2000$  systems. To extract the relaxation time as a function of density of occupied sites,  $\rho$ , temperature,  $T$  and flow velocity,  $v$ , we calculate the persistence function,  $p(t)$ , defined as the probability that a particle has not moved over a time interval  $t$  [13]. At long waiting times we find either exponential  $p(t) = \exp(-t/\tau)$  or stretched exponential  $p(t) = \exp[-(t/\tau)^\beta]$  behavior, depending on density. We extract the relaxation time  $\tau$  from the time at which  $p(t) = 1/e$ .

In the absence of temperature or driving, relaxation slows down with increasing density not only because each particle is more likely to be blocked by its neighbors but also because these neighbors are in turn blocked by their neighbors and so on. Hence moving a particle requires a collective motion of many other particles. In the spiral model the size of blocking clusters is expected to diverge as  $\log(L) \sim (\rho_c - \rho)^{-\mu}$  when

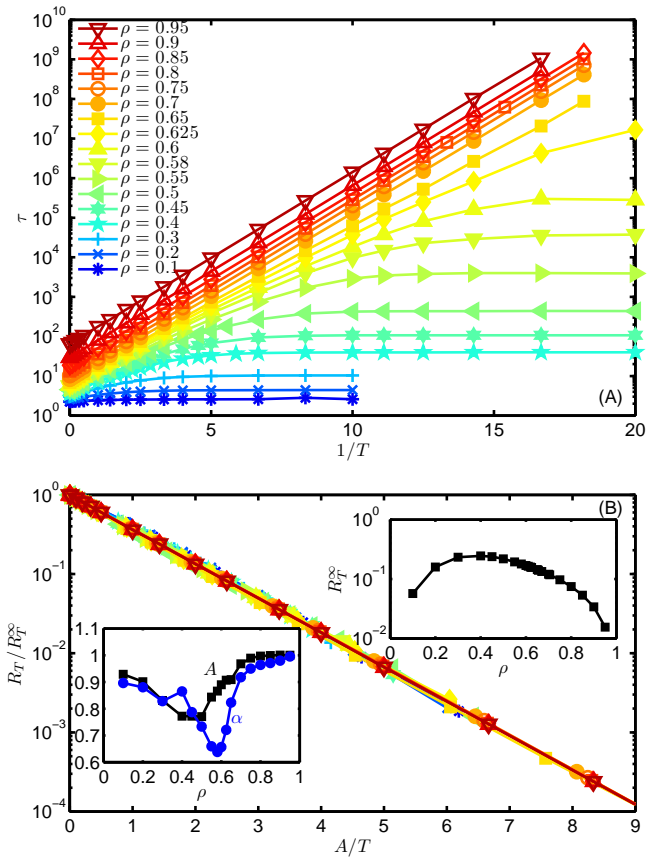


FIG. 2: (Color online) A) Relaxation time vs inverse temperature for various densities. B) Relaxation rate due to the temperature mechanism at all densities may be collapsed to Arrhenius form by normalizing  $R_T$  by its  $T = \infty$  value given in the top inset, and scaling  $T$  by the effective barrier height  $A(\rho)$  given in the bottom inset.

$\rho \rightarrow \rho_c$  [6, 7], and we indeed find behavior which is consistent with  $\log(\tau) \sim (\rho_c - \rho)^{-\nu}$  with  $\nu \approx 1.1$  (see Fig. 1C).

The behavior of the relaxation time as a function of density and temperature at zero driving is summarized in Fig. 2A. As  $T \rightarrow 0$ ,  $\tau$  diverges for  $\rho > \rho_c$ , while for  $\rho < \rho_c$  it saturates to the finite  $T = 0$  value given in Fig. 1C. The singularity at  $\rho_c$  and  $T = 0$  affects the behavior of  $\tau(\rho, T)$  nearby. However, the overall relaxation rate we measure arises from a combination of two types of physical processes, which may be attributed to density and temperature separately. We demonstrate this by writing the relaxation rate as  $1/\tau(\rho, T) = R_\rho(\rho) + R_T(\rho, T)$ . Here,  $R_\rho = 1/\tau(\rho, T = 0)$  is the relaxation rate due to the *density mechanism*, which represents processes subject to the kinetic constraints in which the neighborhood of a particle changes so that a previously-blocked particle can move. Thus,  $R_\rho = 0$  for  $\rho \geq \rho_c$ . Similarly,  $R_T$  is the relaxation rate due to the *temperature mechanism*, representing the process in which a blocked particle moves either by directly overcoming the kinetic constraint or by becoming unblocked when one of its neighbors overcomes its kinetic constraint by thermal activation.

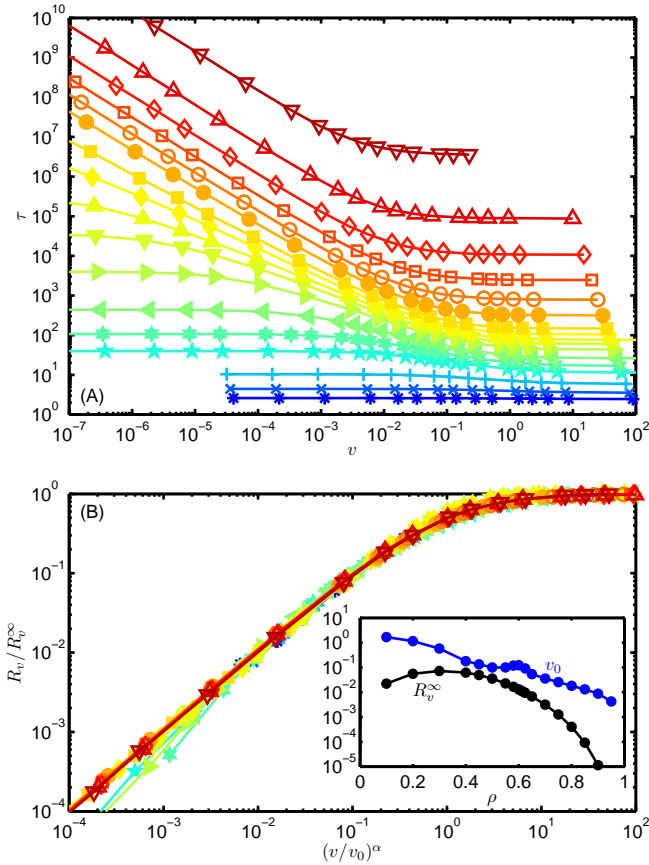


FIG. 3: (Color online) A) Relaxation time vs driving for various densities (same legend as Fig. 2). B) Collapse of relaxation rate due to the driving mechanism for all densities by scaling  $R_v$  by the  $v = \infty$  value and scaling by  $(v/v_0)^\alpha$ .  $R_v^\infty(\rho)$  and  $v_0(\rho)$  are given in the inset and  $\alpha(\rho)$  is given in Fig. 2B.

Clearly,  $R_T = 1/\tau(\rho, T) - 1/\tau(\rho, T = 0)$ . Figure 2B shows that  $R_T$  has a simple Arrhenius dependence on temperature:  $R_T = R_T^\infty \exp(-A(\rho)/T)$ . Here,  $R_T^\infty(\rho)$  is the relaxation rate at  $T = \infty$ , where the kinetic constraint becomes irrelevant. For  $\rho > \rho_c$ , the dominant process facilitated by thermal activation is motion of a single blocked particle moving at probability  $\exp(-1/T)$ , therefore  $A(\rho) = 1$ . For  $\rho \lesssim \rho_c$ , on the other hand, the density and temperature mechanisms are inherently coupled since moves are typically blocked by a large cluster of neighbors, and there are multiple moves that can lead to unblocking a single particle. These collective rearrangements lead to  $A(\rho) < 1$ . Such collective behavior only for  $\rho < \rho_c$  and not for  $\rho > \rho_c$  is another manifestation of the mixed (or one-sided) nature of the jamming transition.

Figure 3A shows the relaxation time vs driving for various densities at zero temperature. We now write  $1/\tau(\rho, v) = R_\rho(\rho) + R_v(\rho, v)$ , where  $R_v$  is the relaxation rate due to the *driving mechanism*, in which the neighborhood of a blocked particle changes due to driving events that unblock it and enable it to move subject to the kinetic constraint. We obtain  $R_v$  by subtracting  $R_\rho$  from  $1/\tau$  and show in Fig. 3B that  $R_v/R_v^\infty$

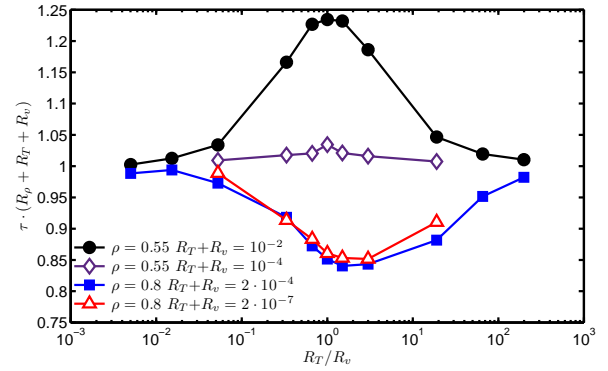


FIG. 4: (Color online) Ratio of the simulated to predicted relaxation time vs ratio of temperature to driving relaxation rates.

has the same dependence on  $(v/v_0)^\alpha$  for all  $\rho$ , where  $R_v^\infty(\rho)$  describes the relaxation rate at infinite driving strength,  $v_0(\rho)$  decreases monotonically with  $\rho$ , and  $\alpha(\rho)$  behaves similarly to  $A(\rho)$  (see insets to Figs. 2B and 3B). Note that above  $\rho_c$  and at densities below  $\rho_c$  but away from the vicinity of the transition,  $\alpha \approx 1$ . Thus,  $R_v$  varies linearly with the flow velocity,  $v$ , at small  $v$ , as one would expect. At higher  $v$ ,  $R_v$  crosses over to a constant at  $v \approx v_0$  because the neighborhood around a particle is completely randomized between attempts of diffusive moves. As a result, increasing the driving strength even more does not affect the relaxation rate at high flow rates.

We now consider the interplay between the temperature and driving mechanisms. Above, we identified the thermal relaxation rate,  $R_T$ , for  $v = 0$ , and the driving relaxation rate,  $R_v$ , for  $T = 0$ . The simplest assumption for nonzero  $T$  and  $v$  is that  $R_T$  does not depend on  $v$ ,  $R_v$  does not depend on  $T$ , and the relaxation rates are additive, so that  $\tau = 1/[R_\rho(\rho) + R_T(\rho, T) + R_v(\rho, v)]$ . Figure 4 shows the ratio of the actual relaxation time measured in simulations in which both  $T > 0$  and  $v > 0$  to this prediction. Obviously, when the values of  $R_T$  and  $R_v$  are very different, the smaller rate becomes irrelevant and the larger behaves as it behaves in the complete absence of the smaller. When  $R_T$  and  $R_v$  are comparable, deviations of around 20% are seen, indicating that the two mechanisms are coupled and the relaxation is not given as a simple sum of independent relaxations. For  $\rho < \rho_c$ , these deviations disappear for small values of  $R_T + R_v$  since then the density mechanism dominates.

Differences between the relaxation mechanisms are also visible in spatial correlations of the dynamics [14]. We measure the dynamic heterogeneity by calculating the variance of the persistence function  $\chi_4(t) = N[\langle p^2(t) \rangle - \langle p(t) \rangle^2]$ , where  $N$  is the number of particles in the system and  $\langle \rangle$  denotes an average over different stochastic realizations for the initial state and dynamics of the system. For given  $\rho$ ,  $T$  and  $v$ ,  $\chi_4(t)$  is maximal roughly when  $t = \tau$  with a value related to the typical number of particles that rearrange collectively [15]. Figure 5 shows the maximal value of  $\chi_4$  vs relaxation time along different paths in the jamming phase diagram. Solid circles

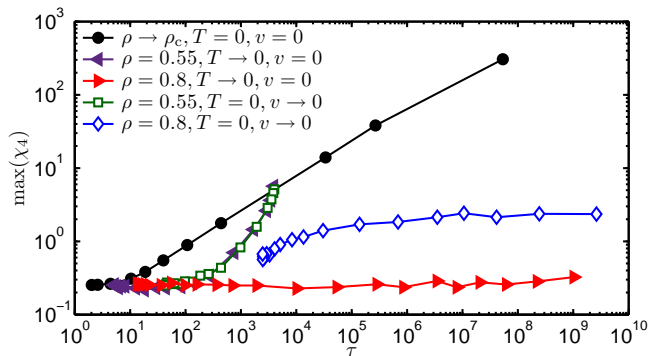


FIG. 5: (Color online) Dynamic heterogeneity vs relaxation time along various paths to jamming.

denote the the path of increasing density at  $T = 0$  and  $v = 0$ . Along this path, the typical size of clusters rearranging collectively diverges, as expected [7], as the system jams. However, when  $T$  decreases at fixed density,  $\chi_4$  does not diverge; the typical spatial size of each rearrangement does not increase as the dynamics become slower. For  $\rho < \rho_c$  both the density and temperature mechanisms are relevant and  $\chi_4$  grows until it meets the  $T = 0, v = 0$  curve (left-pointing triangles). However, for  $\rho > \rho_c$ , relaxation occurs only due to temperature. Such relaxation involves primarily a single blocked particle that waits a long time until it manages to move by a thermal move, and does not rely on the correlated dynamics of many particles. As a result,  $\chi_4$  does not grow at all with decreasing temperature at  $\rho > \rho_c$  (right-pointing triangles).

We now consider a path in which the driving is lowered at fixed density  $\rho < \rho_c$  and fixed  $T = 0$  (open squares in Fig. 5). In this case, both the density and driving mechanisms cause relaxation, and  $\chi_4$  grows until it meets the  $T = 0, v = 0$  curve as for the thermal case. For a path in which driving is lowered at fixed  $\rho > \rho_c$  and fixed  $T = 0$ , on the other hand, the density mechanism is frozen out and relaxation is due to driving alone. As discussed earlier, the primary mechanism for relaxation in that case is that a blocked particle eventually becomes unblocked when its environment is changed by flow. Like the temperature relaxation mechanism, this is a local process that does not become collective as the system jams. Figure 5 shows that indeed  $\chi_4$  is slightly larger than along the  $T \rightarrow 0$  paths than for the thermal case since more particles are involved in each rearrangement event, but the size of such events does not grow with increasing  $\tau$  (open diamonds).

In conclusion, we have introduced a kinetically-constrained lattice-gas with a nontrivial jamming phase diagram. Our model is substantially simpler than currently-used particulate models with more realistic interactions, and is easier to study numerically so that a wide range of time scales may easily be probed even in large systems. In more realistic particulate systems the same physical mechanisms should come into play. However, they will be intermingled in a more complicated way. For example, decreasing temperature in a system with a realistic pair-potential also decreases the ability to open up free volume, and hence effectively increases the

density. It also increases the effective particle diameter and hence the density. These effects lead to non-Arrhenius behavior. Nonetheless, at sufficiently high densities, the density mechanism should eventually freeze out, leading to relaxation primarily by temperature and/or driving. In that regime, our results would suggest that the spatial scale of dynamic heterogeneities should be limited, even at low temperature or driving rates. In fact, analysis of experiments suggests that the increase in the spatial extent of kinetic heterogeneities with decreasing temperature is quite modest in several glass-forming liquids [16], consistent with our results.

We thank Jean-Louis Barrat, Eli Eisenberg, Tom Haxton, Randy Kamien, Carl Modes, David Mukamel, Chris Santangelo, Marija Vucelja, and Ning Xu for helpful discussions. This work is supported by NSF MRSEC grant DMR-0520020 and DE-FG02-05ER46199.

- 
- [1] A.J. Liu and S.R. Nagel, *Nature (London)* **396**, 21 (1998).
  - [2] D.J. Durian, *Phys. Rev. Lett.* **75**, 4780 (1995).
  - [3] C.S. O'Hern, S.A. Langer, A.J. Liu, and S.R. Nagel, *Phys. Rev. Lett.* **88**, 075507 (2002); C.S. O'Hern, L.E. Silbert, A.J. Liu, and S.R. Nagel, *Phys. Rev. E* **68**, 011306 (2003).
  - [4] Similar mixed-nature transitions are known in glasses, see e.g. T.R. Kirkpatrick, D. Thirumalai, and P.G. Wolynes, *Phys. Rev. A* **40**, 1045 (1989).
  - [5] G.H. Fredrickson and H.C. Andersen, *Phys. Rev. Lett.* **53**, 1244 (1984); W. Kob and H.C. Andersen, *Phys. Rev. E* **48**, 4364 (1993); F. Ritort and P. Sollich, *Adv. in Phys.* **52**, 219 (2003).
  - [6] G. Biroli and C. Toninelli, *Eur. Phys. J. B.* **64**, 567 (2008).
  - [7] C. Toninelli, G. Biroli, and D.S. Fisher, *Phys. Rev. Lett.* **96**, 035702 (2006). See also M. Jeng and J. M. Schwarz, *Phys. Rev. Lett.* **98**, 129601 (2007); C. Toninelli, G. Biroli, and D.S. Fisher, *Phys. Rev. Lett.* **98**, 129602 (2007).
  - [8] M. Jeng and J. M. Schwarz, *J. Stat. Phys.* **131** 575 (2008).
  - [9] Note that our driving differs from non-isotropic attempt rates of moves that are subject to the kinetic constraint [10, 11]. Such driving would not unjam the spiral model at  $\rho > \rho_c$ .
  - [10] S.M. Fielding, *Phys. Rev. E* **66**, 016103 (2002).
  - [11] M. Sellitto, *Phys. Rev. Lett.* **101**, 048301 (2008).
  - [12] For mechanical systems, stress is used as the non-equilibrium axis in the jamming phase-diagram, and there is a jammed region below the yield stress. In our model we set the flow rate and do not try to assign the stress required to generate it. Hence, the jammed phase in Fig. 1A reduces to a line.
  - [13] In order to correctly measure relaxation in the presence of driving, the persistence function is defined only in terms of motion along the direction perpendicular to the driving.
  - [14] S.C. Glotzer, *J. Non-Cryst. Solids* **274**, 342 (2000); S. Franz, R. Mulet, and G. Parisi, *Phys. Rev. E* **65**, 021506 (2002); O. Dauchot, G. Marty, and G. Biroli, *Phys. Rev. Lett.* **95**, 265701 (2005); A.S. Keys, A.R. Abate, S.C. Glotzer, and D.J. Durian, *Nature Physics* **3**, 260 (2007).
  - [15] C. Toninelli, M. Wyart, L. Berthier, G. Biroli, and J.P. Bouchaud, *Phys. Rev. E* **71**, 041505 (2005); A. R. Abate and D. J. Durian, *Phys. Rev. E* **76**, 021306 (2007).
  - [16] L. Berthier et al., *Science* **310**, 1797 (2005); C. Dalle-Ferrier et al., *Phys. Rev. E* **76**, 041510 (2007).